# ENERGY AND EXERGY EFFICIENCY OF A HEAT STORAGE UNIT FOR BUILDING HEATING

Mejdi. Hazami[1,*], Sami. Kooli[1], Meriem. Lazâar[1], Abdelhamid. Farhat[1], Ali. Belghith[2]
[1]Laboratoire de Maîtrise et des Technologies de l'Energie, Technopole de Borj Cedria, LP 95 Hammam-Lif, e-mail Hazamdi321@yahoo.fr
[2]Facultée des Sciences de Tunis, université campus, Belvédère, Tunis. 1060

**ABSTRACT.** This paper deals with a numerical and experimental investigation of a daily solar storage system conceived and built in Laboratoire de Maitrise des Technologies de l'Energie (LMTE, Borj Cedria). This system consists mainly of the storage unit connected to a solar collector unit. The storage unit consists of a wooden case with dimension of 5 $m^3$ (5m x 1m x 1m) filed with fin sand. Inside the wooden case was buried a network of a polypropylene capillary heat exchanger with an aperture area equal to 5 m². The heat collection unit consisted of 5 $m^2$ of south-facing solar collector mounted at a 37° tilt angle. In order to evaluate the system efficiency during the charging period (during the day) and discharging period (during the night) an energy and exergy analyses were applied. Outdoor experiments were also carried out under varied environmental conditions for several consecutive days. Results showed that during the charging period, the average daily rates of thermal energy and exergy stored in the heat storage unit were 400 and 2.6 W, respectively. It was found that the net energy and exergy efficiencies in the charging period were 32 % and 22 %, respectively. During the discharging period, the average daily rates of the thermal energy and exergy recovered from the heat storage unit were 2 kW and 2.5 kW, respectively. The recovered heat from the heat storage unit was used for the air-heating of a tested room (4m x 3m x 3m). The results showed that 30 % of the total heating requirement of the tested room was obtained from the heat storage system during the whole night in cold seasons.

## NOMENCLATURE

| | |
|---|---|
| $A_c$ | the surface area of the collector, $m^2$ |
| $A_d$ | the surface area of doors, $m^2$ |
| $A_g$ | the surface area of glasses of windows, $m^2$ |
| $A_s$ | the surface area of the solar storage unit, $m^2$ |
| $A_w$ | the surface area of walls, $m^2$ |
| $A_g$ | the surface area of glass, $m^2$ |
| $A_{Ri}$ | Internal roof surface, $m^2$ |
| $C_{p,\,a}$ | Specific heat of air at constant pressure, kJ/kg K |
| $C_{p,c}$ | the specific heat of concrete absorber, J/(kg K) |
| $C_p$ | the water specific heat, J. $kg^{-1}.K^{-1}$ |
| $C$ | the water specific heat, J. $kg^{-1}.K^{-1}$ |
| $D$ | diffusive intensity of radiation |
| $d$ | diameter of the capillary heat exchanger, m |
| $F$ | lighting coefficient (F =1.2 for florescent lamps and 1 for others) |
| $H$ | is the solar irradiation at the collector aperture, $W.m^{-2}$ |
| $h_i$ | heat transfer coefficient, $W/m^2$ .°C |
| $h_{iR}$ | heat transfer coefficient of the air under the roof, $W/m^2$ .°C |
| $L$ | Length of the capillary tube, m |

| | |
|---|---|
| $M_c$ | Concrete mass, kg |
| $\dot{m}_a$ | Air mass flow rate, kg/s |
| $\dot{m}_w$ | Flow rate of the charging water, $m^3.s^{-1}$ |
| $P$ | Power consumption for lighting system, W |
| $Q_{Charging}$ | Rate of heat supplied from the collector, *W* |
| $Q_{Discharging}$ | Rate of heat supplied from the accumulator, *W* |
| $Q_d$ | Rate of heat recovery from the heat accumulator, *W* |
| $Q_{Loss}$ | Rate of heat loss from the accumulator, *W* |
| $Q_{Storage}$ | the rate of heat stored into the accumulator, *W* |
| *Ss* | Accumulator surface area, *m²* |
| $T_a$ | Ambient air temperature, °C |
| $T_{Abs,av}$ | Average concrete temperature, °C |
| $T_{a,av}$ | Average ambient air temperature, °C |
| $T_{e,av}$ | Average cold-water inlet temperature, °C |
| $T_F$ | Final temperature of the water at the solar storage exit after 12 h, °C |
| $T_I$ | Initial temperature of the water in the tank, °C |
| $T_i$ | Water inlet temperature, °C |
| $T_m$ | Soil temperature inside the accumulator, °C |
| $T_o$ | Water outlet temperature, °C |
| $T_{Ri}$ | Temperature of the internal roof surface, °C |
| $T_s$ | Soil temperature inside the greenhouse, °C |
| $T_{wi}$ | Temperature of the interior surface of the wall, °C |
| $t$ | Time, s |
| $\dot{V}$ | Volumetric flow rate of air, $kg.s^{-1}$ |
| $\eta_{Charging}$ | Net energy efficiency for charging period, *%* |

**Greek letters**

| | |
|---|---|
| $\alpha$ | Absorption coefficient |
| $\rho$ | Water density, $kg.m^{-3}$ |
| $\tau$ | Transmittance for solar radiation. |
| $\lambda_s$ | the equivalent heat conduction coefficient, $W.m^{-1}K^{-1}$ |
| $v$ | the kinematic fluid viscosity |
| $\tau_G$ | transmission coefficient of glass for direct solar radiation |
| $\tau_D$ | transmission coefficient of glass for diffuse solar radiation |

## 1. INTRODUCTION.

Energy constitutes the main element of economical production (in industry and transportation) and improving life quality in the residence sector. In fact, approximately 50% of the annual energy consumption of primary energy resources throughout the world is destined to household air-conditioning. Furthermore, the over-use of primary energy is leading to environmental degradation in heavily populated areas. Thus, actually wide efforts have been undertaken to alleviate global warming of earth caused by the emission of carbon dioxide in atmosphere generated by intensive burning of fossil fuels. Due to these problems, tendency towards renewable energy resources, particularly solar energy, with rather insignificant environmental influences, offers wide range of exceptional benefits for air-houses heating. Indeed, solar energy, which is an abundant, clean and safe source, is an attractive substitute for conventional fuels for passive and active heating. However, the management of the solar energy in air-heating sector is usually not economically feasible compared with the traditional

carriers. In fact, its intermittent character constitutes the main impediment of solar energy use. To reduce the time or rate mismatch between energy supply and energy demand it is necessary to store the excess of solar heat for short-or long-term storage. The short-or long-term storage of the sensitive heat in soil seems to be plausible from a technical and economic view point. Indeed, different techniques of storage of the sensitive heat in soil have been used (OOzt.urk et al., 2002). The performances of these techniques are influenced by the transfer of the heat, of the humidity in soil and the thermal efficiency of the heat exchanger used for storing solar heat in soil. T. Boulard and A. Baille (1986) analyzed the influence of some parameters on the performances of a thermal energy storage system. This system consists of a 10 cm-diameter PVC heat exchanger tubes buried in soil at 30 cm-depth connected to an air-ventilation system placed inside a greenhouse. Results showed that the storage of heat by through the buried air/soil heat exchanger was an interesting method that can be used for the daily solar heat storage. In fact, the thermal efficiency of the solar heat storage system was evaluated at 50%. In 1997, Gauthier et al., proposed a three-dimensional numeric model, using the FLUENT program, to study the performances of a water/soil heat exchanger used to store heat collected from greenhouse. The heat storage system consists mainly of two connected tubular heat exchangers. The first heat exchanger is placed inside the greenhouse. The second heat exchanger is buried within the underground of the same greenhouse. The heat collected from the first heat exchanger is transferred to the second heat exchanger buried in the underground. The results showed that the thermal transfer in the ground due to the pressure gradients of humidity in soil is insignificant when compared to the heat transfer due to the temperature of gradients. Results showed that the storage of heat by through the buried air/soil heat exchanger was an interesting method that can be used for the daily solar heat storage. Gauthier and al. established that the thermal efficiency of the heat storage system is about 60%. In this context, we have built in our laboratory (LMTE, Borj Cedria), a prototype for sensible solar energy storage (Figure 1). The experimental system consists mainly of (i) a solar storage unit which consists of a wooden casing whit dimension of 5 $m^3$ filed with fin sand. Inside the solar storage unit was buried a network of a polypropylene capillary heat exchanger with an aperture area equal to 5 $m^2$ and (ii) a solar collector unit with an aperture area of 5 $m^2$ connected to a buried heat exchanger. An experimental study was carried out in order to evaluate the thermal performances of the storage system. Performances of the heat storage system was evaluated by a theoretical analyzes based on first and second law of thermodynamics.

Figure 1: Photo of the solar heat storage unit

From a first law perspective, the efficiency of a thermal energy storage system was assessed in terms of how much thermal energy the system can store. This approach produces workable designs, but not

necessarily those with the highest possible thermodynamic efficiencies. It has been shown in recent years that the design of thermodynamically efficient heat transfer equipment must be based on the second law of thermodynamics in addition to the first law (Krane, 1987). Exergy analysis, derived from both the first and second laws of thermodynamics, provide greater insight to cost effective design and management of complex processes (Larson & Cortez, 1995). Unfortunately, there are only a few publications related to exergetic efficiency of the large-scale heat storage applications. The endeavor of this paper is to appraise the performances of this low cost storage system studied under various Tunisian climatic conditions using energy and exergy analyzes. The energy and the exergy analyzes established in this paper allowed the estimation of the maximal value of heat stored inside the heat storage unit.

## 2. EXPERIMENTAL INVESTIGATION

**2.1. Experimental device** Figure 2 illustrates a schematic diagram of the solar heat stored system. The system consists of three units: (i) heat collection unit, (ii) heat storage unit and (iii) data acquisition unit.

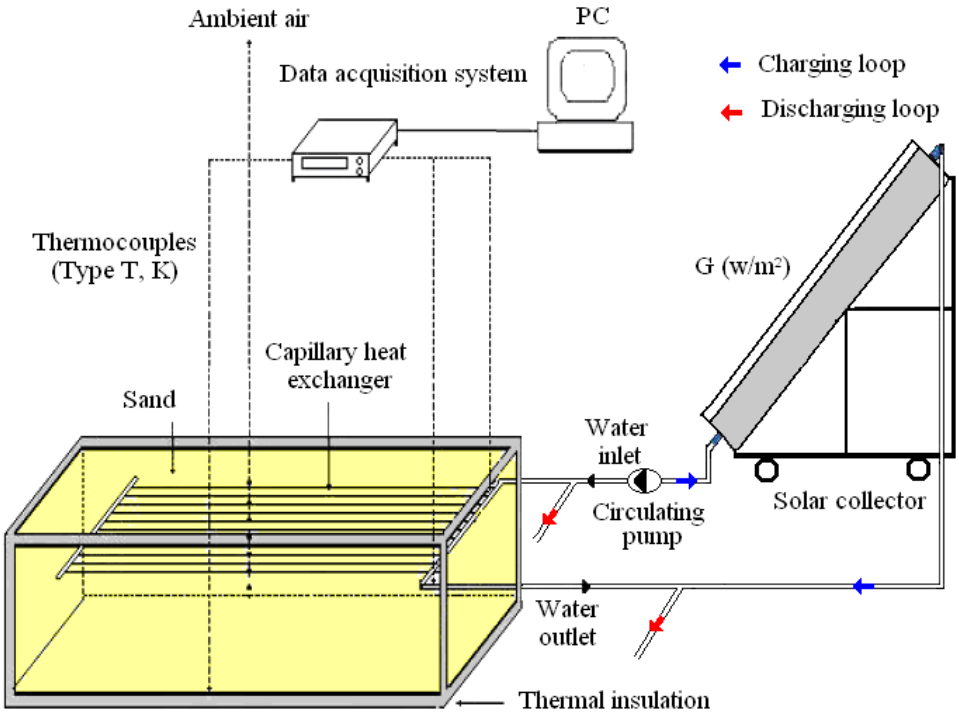


Figure 2: Solar heat storage system

*2.1.1. Heat collection unit* The heat collection unit is composed of a solar collector with an aperture area of 5 m² mounted at 37° towards the south. The absorber of the solar collector was made with 40-cm thick concrete slab painted black. The concrete matrix was used to increase the storage capacity of the heat collection unit. The thermophysical and geometrical proprieties of the absorber are given in table 1. A capillary polypropylene heat exchanger (*Figure 3*) with an aperture area equal to 5 m² was being integrated inside the absorber matrix to carry the heat transfer fluid inside the solar storage collector. The thermophysical and geometrical proprieties of the heat exchanger are given in table 2.

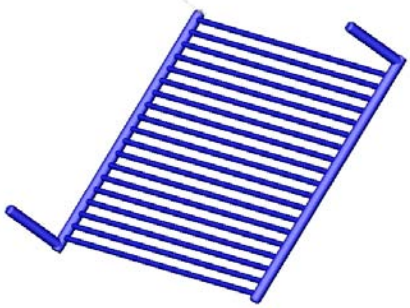

Figure 3: Capillary heat exchanger

Table 1
Physical and geometrical proprieties of the heat collection unit

| Parameters | Value |
|---|---|
| Dimensions | (1 m x 5 m) |
| Collector price | 90 ($/1m) |
| Absorber material | Concrete |
| Concrete mass | 200 kg |
| Concrete density | 2800 $kg.m^{-3}$ |
| Concrete thermal conductivity | 0.81 $W.m^{-1}.K^{-1}$ |
| Concrete specific heat | 880 $J.kg^{-1}.K^{-1}$ |
| Toxic effect | No |

Table 2
Physical and geometrical proprieties of the capillary heat exchanger

| Parameters | Value |
|---|---|
| Dimensions | (1 m x 5 m) |
| Inner capillary | 3 mm |
| Outer diameter | 4.2 mm |
| Heat exchanger price | 20 ($/1m) |
| Heat exchanger material | Polypropylene |
| Polypropylene density | 950 $kg.m^{-3}$ |
| Polypropylene thermal conductivity | 0.22 $W.m^{-1}.K^{-1}$ |
| Toxic effect | No |

*2.1.2. Heat storage unit* A wooden case of a 5m length, 1m width and 1 m depth, field with fin sand, was used as a heat storage unit. The sand characterized by a high storage capacity per unit volume was used as a heat storage material. The whole surface of the heat storage unit was insulated with 30-mm of polyurethane foam. A network of a polypropylene capillary heat exchanger with 5 m² aperture area is buried within the sand inside the case at 40 cm-depth. In fact, preliminary experiment was carried out on the storage unit in order to determine the optimal depth in which the heat exchanger will be buried. The test consisted of following the variation of the sand temperature at different depths vs time. By analyzing the results we noticed that the superior layers of sand undergoes easily with the external climatic variation. Beyond a certain depth, the sand temperature does not vary between the day and the night. Thus sand inside the storage unit can be divided into two zones (upper and lower). The thickness of the upper zone is about 20 cm. In this zone, the sand temperature fluctuates seriously with external climatic conditions. Under this depth

the sand temperature dose not oscillates with external climatic conditions. Thus, less than 20 cm-depth is considered to be a long-term thermal storage section.

*2.1.3. Data acquisition unit* Measurements made during the experimental studies are divided into to groups:

-The first group measurements are related with the heat collection unit. Both the collector outlet temperature $T_{co}$ and collector inlet temperature $T_{ci}$ have been measured by T-type thermocouples.

-Second group measurements are concerned with the sand in the wooden case and the temperature value of the surrounding ground. Thus, copper-constantan T-type thermocouples were placed at different depths inside the sand at 10, 20, 30, 40, 50, 60, 70, 80, 90 and 100 cm depth on the central line. The inlet temperature $T_{so}$ and the outlet temperature $T_{si}$ of the capillary heat exchanger integrated inside the sand have been measured.

The ambient air temperature was measured by another thermocouple placed out of the system. A pyrometer has been used to measure the global radiation coming towards the horizontal surface. All the thermocouples used were new and of high accuracy. The data measured were recorded every 15 mm with a total accuracy assumed to be about 5% by a *HP* data logger and then transferred to a *PC* for further evaluation.

**2.2. Experimental protocol** An experimental investigation were conduced in Borj Cedria (North of Tunisia): Latitude 36° 50' N, Longitude 10 ° 44' E. The experimental study was elaborated in two complementary stages:

*(i) First stage (A storage phase)*

The experiments were carried out at the same time periods between 9.00 and 17.00 of the days for a mass flow rate maintained equal to 0.0416 kg.s$^{-1}$ by using the sliding valve integrated at the experimental loop. During this phase the heated water (at the temperature rang of 40-50°C) supplied by the heat collection unit, is conduced thought the polypropylene heat exchanger buried at 40 cm depth inside the sand. The hot water inside the heat exchanger dissipates its thermal energy to the sand inside the case by conduction.

*(ii) Second stage (A restoration period)*

The heat stored in the accumulator during the charging period was recovered during the nights (20:00–03:00 h). During the discharging phase cold water, at a temperature and masse flow equal to 20 °C and to 0.0416 kg.s$^{-1}$ respectively, replenish thought the heat exchanger buried in the sand. The hot sand inside the case dissipates the stored solar energy to the buried heat exchanger.

## 3. NUMERICAL STUDY

**3.1. Solar collector unit** According to the INPUT/OUTPUT standard (Hikmet (2008)), the energy gain (daily heat output) of the solar collector, $Q_u$ (W), can be represented by the following empirical equation:

$$Q_u = \alpha_1 H + \alpha_2 (T_{a,av} - T_{e,av}) + \alpha_3 \quad (1)$$

$\alpha_1$, $\alpha_2$ and $\alpha_3$ are constants for a system, determined from the test results (Table .1).

The overnight heat loss coefficient, $U_c$ (W/K.m²), of the hot water storage system is determined by measuring the temperature loss of the water during a 12 h nocturnal period (Souliotis et al. (2004)). The formula used is:

$$U_C = \frac{M_c C_{p,c}}{A_c \, \Delta t} \ln \frac{T_I - T_{a,av}}{T_F - T_{Abs,av}} \tag{2}$$

The daily thermal efficiency of the solar collector, $\bar{\eta}_j$, is given by the expression:

$$\bar{\eta}_j = \frac{\int_{t1}^{t2} Q_u(t)\, dt}{\int_{t1}^{t2} A_c . H(t)\, dt} \tag{3}$$

The solar collector parameters were determined during an experimentally investigation. Results are shown in Table 3.

Table 3
Collector parametric data

| Parameters | Value |
|---|---|
| Collector overall energy loss coefficient, $U_C$ (W/m².K) | 12 |
| The optical yield, $\eta_0$ | 0.86 |
| $\alpha_1$ ($m^{-2}$) | 30 |
| $\alpha_2$ ($W.K^{-1}$) | 0.35 |
| $\alpha_3$ | -12.7 |
| $\bar{\eta}_j$ (%) | 35 |

**3.2. Heat storage unit**

*3.2.1. Energy analysis for charging and discharging periods* The rate of heat transfer $Q_{Charging}(t)$ from the solar collector unit into the heat storage accumulator was calculated during the charging period by using the following equation:

$$Q_{Charging}(t) = \dot{m}_w C_p (T_i(t) - T_O(t)) \tag{4}$$

The rate of heat stored in the heat storage unit $Q_{Storage}(t)$ was determined with respect to the heat transfer rate into the storage unit and heat losses for the charging period:

$$Q_{Storage}(t) = Q_{Charging}(t) - Q_{Losses}(t) \tag{5}$$

$Q_{Losses}(t)$ represents the rate of heat loosed from the whole surface area of the heat storage unit. It is given by the relation:

$$Q_{Losses}(t) = \lambda_s A_S (T_m(t) - T_s(t)) \tag{6}$$

The evaluation of the sand temperature $T_S(t)$ during the charging and the discharging periods, is obtained by the resolution of the equation of the heat conduction:

$$\rho c \frac{\partial T_S}{\partial t} = \frac{\partial}{\partial x}(\lambda_s \frac{\partial T_S}{\partial x}) + \frac{\partial}{\partial y}(\lambda_s \frac{\partial T_S}{\partial y}) \quad (7)$$

The sand temperature, $T_S(t)$, was determined by the heat conduction equation (S. V. Patankar, 1980). To resolve the heat conduction equation, the following simplifying assumptions were taking into account; (i) The ground was regarded as being homogeneous and (ii) The convective coefficient, h, was supposed to be constant throughout the heat exchanger embedded inside the sand. The integration of the heat conduction equation (Between t at t+Δt) gived the equation:

$$a_P T_P = a_E T_E + a_W T_W + a_N T_N + a_S T_S + a_P{}^0 T_P{}^0 \quad (8)$$

Where:

$a_E = \frac{\lambda_s)_e \Delta y}{\partial x_e}$, $a_W = \frac{\lambda_s)_W \Delta y}{\partial x_W}$, $a_N = \frac{\lambda_s)_n \Delta y}{\partial x_n}$, $a_S = \frac{\lambda_s)_S \Delta y}{\partial x_S}$, $a_S = \frac{\lambda_s)_S \Delta y}{\partial x_S}$, $a_P{}^0 = \frac{\rho c \Delta x \Delta y}{\Delta t}$

and $a_P = a_E + a_W + a_N + a_S + a_P{}^0$

The corresponding boundary conditions are:

$-\lambda_s \frac{\partial T_S}{\partial x}/_{x=0} = 0$ ; $-\lambda_s \frac{\partial T_S}{\partial x}/_{x=L} = 0$ ; $-\lambda_s \frac{\partial T_S}{\partial x}/_{y=0} = 0$ ; $-\lambda_s \frac{\partial T_S}{\partial x}/_{y=l} = 0$

$-\lambda_s \frac{\partial T_S}{\partial x}/_{x=k} = h(T_{water} - T_m)$ ; $k$ is the position of the heat exchanger within sand and $h$ represents the heat transfer coefficient between the sand particles and the water in the heat exchanger. The form of the correlation used for the evaluation of the heat transfer coefficient $h$ was developed by R. Kübler, 1987:

$$Nu = 0.023.Pr^{0.33}.Re^{0.8}.\left[1 + \left(\frac{d}{L}\right)^{0.7}\right]$$

The energy efficiency for the charging period was defined as the ratio of the heat stored in the heat storage unit to the heat transfer from the solar heat collector. Then, the total energy efficiency during the charging period $\eta_{Charging}$ (t) in % was formulated as follows:

$$\eta_{Charging}(t) = \frac{Q_{Storage}(t)}{Q_{Charging}(t)}.100 \quad (9)$$

The rate of heat recovered from the heat accumulator during the discharging period: $Q_{Discharging}(t)$ was calculated by:

$$Q_{Discharging}(t) = \dot{m}_w C_p (T_O(t) - T_i(t)) \quad (10)$$

*3.2.2. Exergy analysis for the charging and discharging periods* The rate of thermal exergy transfer from the heat collection unit into the heat storage unit $\dot{X}_C(t)$ in W was calculated during the charging period from the following equation (Öztûrk H H; 1997) :

$$\dot{X}_C(t) = Q_{Charging}(t) - T_{ex}\dot{m}_w C_p Ln\frac{T_i(t)}{T_O(t)} \quad (11)$$

where $T_{ex}$ is the reference outside temperature. It is important to mention that the rate of thermal exergy transfer is usually calculated on the basis of the rate of thermal energy transfer.
The symbol $\dot{X}_C(t)$ refers to the rate of exergy transfer in the literature of thermodynamics. The rate of the thermal exergy stored in the heat storage unit $\dot{X}_S(t)$ was determined in relation to the exergy transfer rate into the heat storage unit and the exergy loosed from the heat storage unit for the charging period:

$$\dot{X}_S(t) = \dot{X}_C(t) - \dot{X}_l(t) \quad (12)$$

where $\dot{X}_l(t)$ is the rate of thermal exergy loosed from the heat storage unit.
During the charging period, the rate of the thermal exergy losses was evaluated as follows:

$$\dot{X}_l(t) = Q_{Charging}(t)\,[1-\frac{T_s(t)}{T_m(t)}] \quad (13)$$

Similarly energy efficiency, the total exergy efficiency during the charging period was determined by the following equation:

$$\psi_c(t) = \frac{\dot{X}_S(t)}{\dot{X}_l(t)}.100 \quad (14)$$

The rate of thermal exergy recovered from the heat storage unit for the discharging period $\dot{X}_R(t)$ was calculated on the basis of the rate of heat recovered from the heat storage unit $Q_{Discharging}(t)$ as follows:

$$\dot{X}_R(t) = Q_{Discharging}(t) - T_{ex}\dot{m}_w C_p Ln\frac{T_0(t)}{T_i(t)} \quad (15)$$

*3.2.3. Heat requirement of the tested room* The total heating load can be calculated by considering into account the effect of various parameters according (T. Hong, Y. Jiang., 1997 et M.S. Hatamipour et al., 2007):

$$Q_P = Q_{Transmission} + Q_{Solar} + Q_{Internal} + Q_{Airflow} \quad (16)$$

$Q_p$ represents the total heat transferred to the room air when water flowing through the polypropylene heat exchanger integrated inside the air-cupboard. It was calculated from the temperature difference between the entrance and the exit of the capillary heat exchanger:

$$Q_p = \dot{m} C_p (T_{w,o} - T_{w,i}) \quad (17)$$

$Q_{Transmission}$ represents the heat transfer from exterior walls, windows, door and envelopes (A. Sharian et al., 1998) :

$$Q_{Transmission} = h_i \sum_{j=1}^{Nw} A_{wj}(T_{wi} - T_a)_j + A_{gj}(T_g - T_a)_j + A_{dj}(T_d - T_a)_j + h_{iR} \sum_{j=1}^{NR} A_{Rj}(T_{Ri} - T_a)_j \quad (18)$$

$Q_{Solar}$ represents the heat due to sun radiation transmitted from windows. Thermal heat due to this phenomenon is calculated by using:

$$Q_{Solar} = \tau_G H + \tau_D D \quad (19)$$

$Q_{Internal}$ represents internal heat generated by lighting system, persons in the building and home appliances can be calculated by using (Y. Jiang, 1981) :

$$Q_{Internal} = Q_{Lihting} + Q_{Persons} + Q_{Appliances} \quad (20)$$

Heat generated by lighting system was calculated by:

$$Q_{Lighting} = P.F \quad (21)$$

Heat generated by persons and appliances were achieved from appropriate tables. $Q_{Airflow}$ is the heat due to airflow into the building (sensible and latent heat). Heat load due to outside air flow infiltration can be calculated by (E. Shaviv et al., 2001):

$$Q_{Airflow} = Q_s + Q_L \quad (22)$$

Where:

$Q_s = \dot{V} \rho c_{p,a} (T_{a,0} - T_{a,i}) = \dot{m}_a \ c_{p,a} (T_{a,0} - T_{a,i})$ (Sensible heat by entering air)

$Q_L = \dot{V} \rho (W_i - W_0) \lambda$ (Latent heat by entering air)

## 4. RESULTS AND DISCUSSION

The efficiency of the heat storage system depends on thermal and physical properties of the heat storage material (*Sand*), heat storage temperature and performances of the heat exchanger embedded inside the sand. In view of evaluating efficiency of the heat storage system, an energetic and an exergetic analyses were evaluated for the following charging/discharging process.

**4.1. Charging process** Figure 4 represents the numerical and experimental variation of the sand temperature at 50 cm-depth during the storage phase (between 9:00 and 17:00). It is found that the temperature of the sand, $T_{S,à}$ inside the case increased gradually with the increased of water temperature supplied by the solar collector. At the end of the charging process the sand temperature, at 50 cm-depth, reached a maximum value about 40 °C. Figure 4 shows also a good agreement between numerical and experimental results. The rates of heat and thermal exergy stored in the heat storage unit during the charging period were calculated by using Eqns (4), (5) and (6), respectively. The results of energy and exergy analyzes during the charging period are shown in Figure 5. Figure 5 shows that the average hourly rate of thermal energy and thermal exergy changed with time. In fact, the rate of the heat stored in the heat storage unit ranged from 400 W to 2.8 kW, whereas the rate of the thermal exergy stored in the heat storage unit was in the range of 300 W and 830 W. The

maximum values of energy and exergy rates (2.6 kW and 830 W respectively) were obtained at 13:30. During the charging period the average daily rates of the heat and thermal exergy stored in the heat storage unit were 515 W and 1.5 kW, respectively. We noted that the thermal energy stored in the heat storage unit was higher compared with the thermal exergy during the charging period. The energy and exergy efficiencies of the heat storage system during the charging period were calculated by using Eqs (9) and (14), respectively. The changes of the average hourly energy and exergy efficiencies during the charging period are shown as a function of time in Figure 6. The energy and exergy efficiencies increased with the temperature increasing of the water supplied by the solar collector. The result shows that during the charging period (10:00 h –17:00 h) the energy efficiency ranged from 23 to 41 %, while the net exergy efficiency was in the range of 17 and 28 %. The energy and exergy efficiencies reach they're maximum values (41 % and 17 % respectively) at 13:30. During the charging period, it was found that the average daily net energy and exergy efficiencies were 32 and 22.5 %, respectively. We noted also that the energy efficiency is higher than the exergy efficiency.

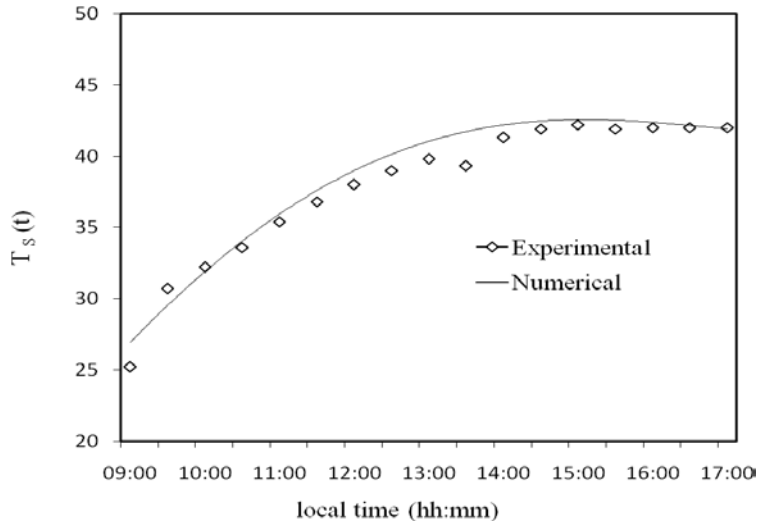


Figure 4: Evolution of the sand temperature at 50 cm-depth during the charging phase

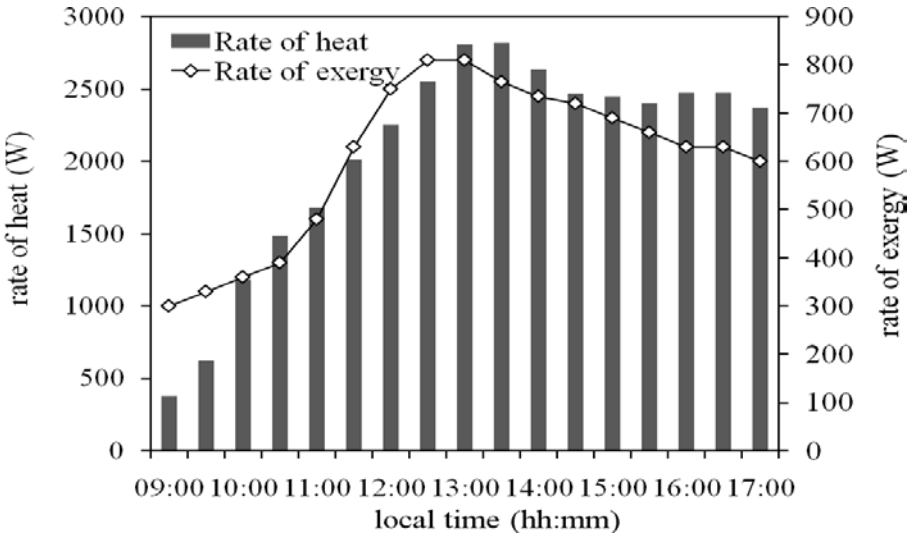


Figure 5: The rates of heat and thermal exergy stored in the heat storage unit during the charging period

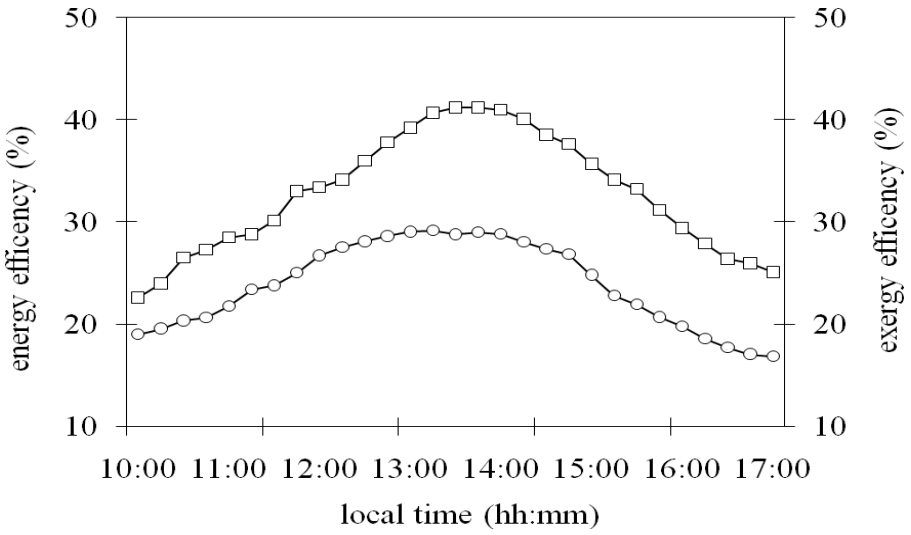


Figure 6: The change of the net energy and exergy efficiencies for the charging period: □, energy efficiency, O exergy efficiency

**4.2. Discharge process** During the discharge process, the temperature distribution of the sand indicated by the 12 thermocouples fixed at different equal intervals depths inside the case filed with sand. Figure 7 shows that the temperature of the sand at 50 cm-depth decreases gradually. The decrease temperature is due to the release of sensible heat stored in sand. During the energy discharging, the sand temperature in the storage heat unit decrease quickly in the first two hours. At the end of the discharging process the sand temperature at 50 cm-depth reached a minimum value about 21 °C. Figure 7 shows also a good agreement between numerical and experimental results. The rates of heat and thermal exergy recovered from the heat storage unit during the discharging period were calculated by using Eqns (10) and (15), respectively. The changes of the average hourly rates of heat and thermal exergy recovered from the heat storage unit during the discharging period are shown as a function of time in figure 8. The amount of heat recovered from the heat storage unit was in the range of 2 kW and 2.5 kW during the discharging period. However, it was found that the thermal exergy recovered from the heat storage unit ranged from 600 W to 900 W. During the discharging period the average daily heat and thermal exergy recovered from the heat storage unit were 2.25 kW and 1500 W, respectively. The results showed also that the difference between energy and exergy analyzes is significant. Since exergy is a measure of the quality of energy, exergy efficiency is more significant than energy efficiency, and that exergy analysis should be considered in the evaluation and comparison of the thermal energy storage systems. Exergy analysis clearly takes into account the loss of availability of heat in storage operations and, hence, it more correctly reflects the thermodynamic and economic value of the storage operation. The optimization of the design and exploitation of the thermal energy storage systems can be made by means of the exergy analysis. When optimizing the efficiency of a thermal energy storage system, both design and operational parameters must be considered.

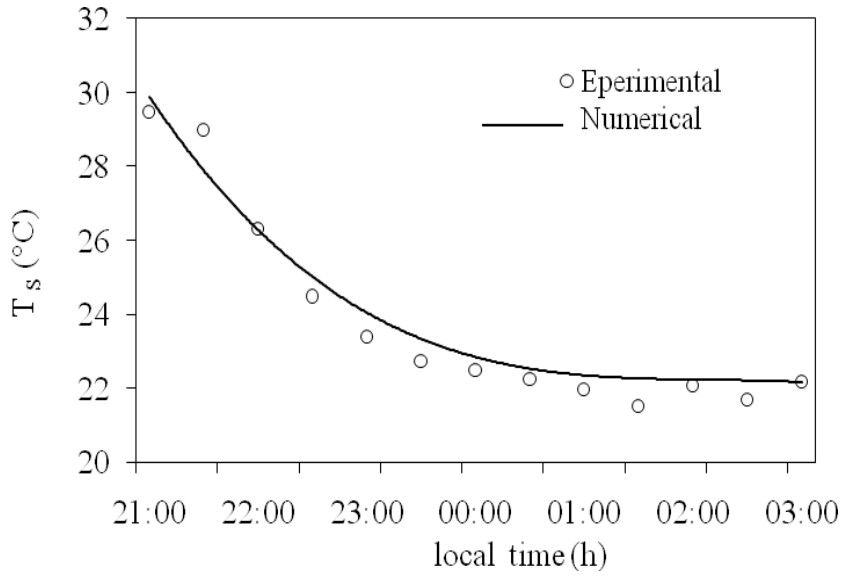


Figure 7: Evolution of the sand temperature at 40 cm-depth during the discharging phase

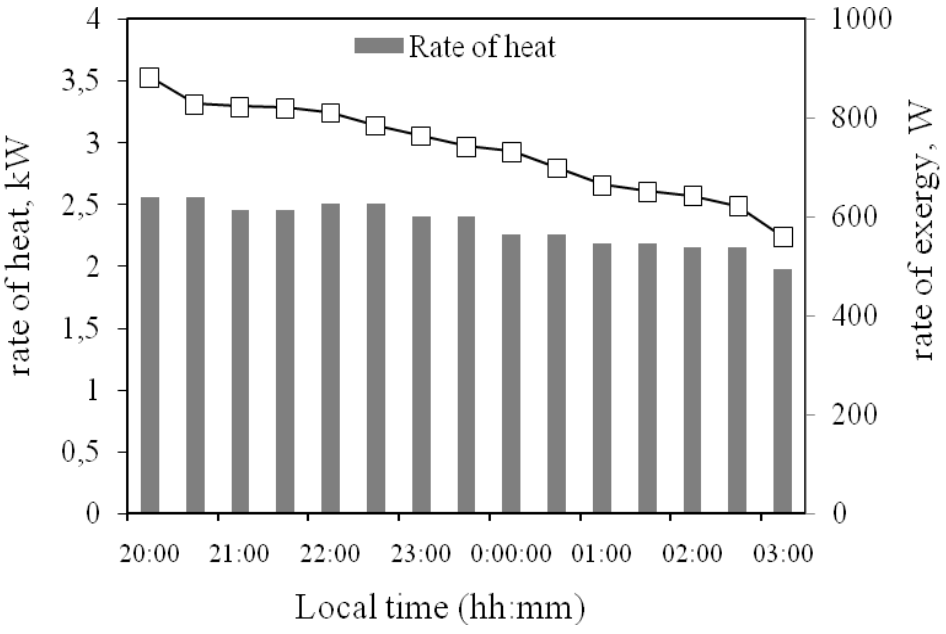


Figure 8: The rates of heat and thermal exergy recovered from the heat storage unit for the discharging period

**4.3. Heat requirement of the tested room** The total heat requirements of the tested room during the discharging period were calculated from Eq (16). The changes of the total heat requirement of the tested room and the amount of heat recovered from the heat storage unit during the discharging period are shown as a function of time in Figure 9. During the discharging period, the total heat requirement of the room ranged from 7.2 to 8.2 kW, while the rate of heat recovered from the heat storage unit to the tested household was in the range of 2 and 2.5 W. We established that about 30 % of the total heat requirement of the tested room was obtained from the heat storage unit.

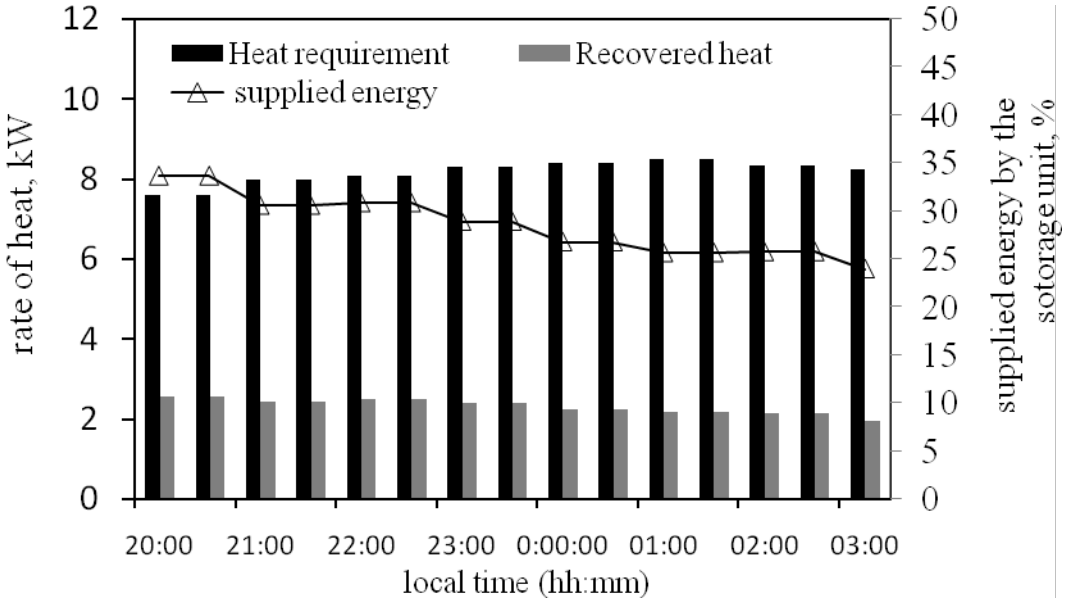


Figure 9: The changes of the total heat requirement of the tunnel greenhouse and the rate of heat recovered from the heat storage unit during the discharging period

## CONCLUSION

The performance of a newly designed heat storage system been presented. Results show that the heat storage system would be a promising solution for air-heating buildings during the night-time. In fact, the heat storage attained a considerable rate of heat stored (about 2.6 kW) with an energy efficiency and exergy efficiency which reached 41 % and 28 %, respectively. We noted also that the amount of heat recovered from the heat storage unit was in the range of 2 kW and 2.5 kW during the discharging period. However, it was found that the thermal exergy recovered from the heat storage unit ranged from 300 W to 800 W. The results showed also that the difference between energy and exergy analyzes is significant. Since exergy analysis clearly takes into account the loss of availability of heat in storage operations and, hence, it more correctly reflects the thermodynamic and economic value of the storage operation. During the discharging period, the total heat requirement of the room was about 8.60 kW, while the rate of heat recovered from the heat storage unit to the tested household evaluated by the numerical study was about 2.5 W. We established that about 30 % of the total heat requirement of the tested room was obtained from the heat storage unit.

## REFERENCES

Boulard, T. and Baille, A. [1986], Simulation and analysis of soil heat storage systems for a solar Greenhouse. *Energy Agric*, Vol. 5, pp 285-293.

Gauthier, C., M. Lacroix and H. Bernier, [1997], Numerical simulation of soil heat exchanger-storage systems for greenhouses, *Solar Energy*, Vol. 60, pp. 333-346

Hatamipour. M. S., Mahiyar. H. and Taheri. M. [2007], Evaluation of exising cooling sustems for reducing cooling power consumption. *Energy and Buildings*. Vol. 39, pp. 105-112.

Hikmet, E. [2008], Experimental energy and exergy analysis of a double-flow solar air heater having different obstacles on absorber plates. *Building and Environment*. Vol. 43, pp. 1046–1054.

Hong, Y. Jiang. [1997], A new multizone model for the simulation of building thermal performance, *Building and Environment*. Vol. 32, No. 2, pp. 123–128.

Jiang, Y. [1981], State space method for analysis of the thermal behavior of rooms and calculation of air-conditioning load, *ASHARE Transactions*. Vol. 88, pp. 122–132.

Krane, R. J. [1987], A second law analysis of the optimum design and operation of thermal energy storage systems, *International Journal of Heat Mass Transfer*, Vol. 30, No. 1, pp. 43–57

Kübler. R., Bierer. M. and Hahne .E. [1987], Heat transfer from finned and smooth tube, heat exchanger coils in hot water stores, *Heat and Mass Transfer*, Vol. 30, No. 14.

Larson, D. L. and Cortez, L. A. B. [1995], Exergy analysis: essential to effective energy management. *Transactions of ASAE*, Vol. 38, No. 4, pp. 1173−1178

Öztûrk, H. H. [1997], The research on storage of solar energy in phase change material (PCM) for greenhouse heating, *PhD Thesis, Department of Agricultural Machinery Institute of Natural and Applied Sciences*, University of -Cukurova, Turkey

Öztûrk. H. H. and Basçetinçelik. A. [2002], Thermal energy storage techniques, *The Union of Turkish Chambers of Agriculture*, Publication Number 230, Ankara

Patankar. S. V. [1980], Numerical heat transfer and fluid flow. Mc Graw-Hill, New York.

Sharian, A., Shalabi B., Rousan A., Tashtoush B.. (1998). Effects of the absorptance of external surfaces on heating and cooling loads of residential buildings in Jordan. *Energy Conversion & Management*. 39 (3/4) 273-284.

Shaviv. E., Yezioro. A. and I. Capelurto, G. [2001], Thermal mass and night ventilation as passive cooling design strategy. *Renewable Energy*. Vol. 24, pp. 445-452.

Souliotis, M. and Tripanagnostopoulos, Y. [2004], Experimental study of CPC type ICS solar systems. *Solar Energy*, Vol. 76, pp. 389–408